[Article ID] 1003- 6326(2002)05- 0845- 05

Atomic simulation of amorphization and crystallization of $Ag_{50}Au_{50}$ alloy during rapid solidification①

WANG Li(王 丽)[1], YANG Hua(杨 华)[1], ZHANG Jun-yan(张均艳)[1],
BIAN Xiu-fang(边秀房)[1], YI Su(衣 粟)[2]
(1. The Key Laboratory of Liquid Structure and Heredity of Materials,
Ministry of Education, Shandong University, Ji'nan 250061, China;
2. Shandong Research and Inspect Institute of Boiler and Pressure Container, Ji'nan 250013, China)

[Abstract] By means of constant temperature and constant pressure molecular dynamic simulation technique, a series of simulations of the glass transition and crystallization processes of $Ag_{50}Au_{50}$ were performed. The atoms interact via EAM potential function. Pair correlation functions of liquid $Ag_{50}Au_{50}$ during different cooling rates and temperatures were simulated to reveal the structural features of liquid, super-cooled liquid, glass state and crystal. The thermodynamics and kinetics of structure transition of $Ag_{50}Au_{50}$ during cooling processes were performed.

[Key words] molecular dynamic simulation; liquid $Ag_{50}Au_{50}$; structural features; thermodynamics and kinetics
[CLC number] TG 146.3 [Document code] A

1 INTRODUCTION

The study on the structure of liquid metals has been receiving the attention experimentally and theoretically. The investigation of experiments indicate that the macroscopic structure of metallic materials depend on their microstructure, and the microstructure is influenced by the structure of melt matrix before solidification. As a consequence, it is an instructive significance for seeking the fine techniques of material solidification and obtaining nice properties to investigate the structural change of liquid metals under different temperatures. However, it is difficult to make an extensive study of liquid with high temperature under normal conditions. Several techniques to obtain the disordered state have been proposed[1]. The rapid solidification has been adopted widely to obtain amorphous phase. However, the high cooling rate restricts the use of the technique. Computer simulation as a method to investigate metallic liquid, super-cooled liquid, glass and crystal certainly have a much shorter history than any other methods since the first work dates back only to the 1950 s[2]. However, it has already been shown that such simulations can be an excellent tool for investigating the properties of complex systems[3], and it can be expected that with the availability of faster and cheaper computers, as well as improved algorithms, such simulations will play an even more important role in the future than they do now.

The interatomic potentials are very important in the MDC(molecular dynamics). Resent years have witnessed considerable progresses in the development of empirical and semiempirical many-body potentials for accurately reproducing thermodynamic and structural properties of most transition metals. The embedded-atom method (EAM) by Daw and Baskes[4,5] (further developed by Johnson[6~8]) has been successfully applied to a wide range of aspects in the solid, such as in the point defects, dislocations and surface[9~11]. However, few reports have involved the liquid metal and their alloys. The microstructure of Au-Ag alloys have attracted much attention over years[12], but a large number of difficulties have to be met because of high price of Au-Ag alloys. It is well known that gold and silver are typical complicated metals. Some interesting structures may appear when they are mixed together. However, the interatomic potential about Au-Ag alloys is unknown. The purpose of this work is to develop the interatomic potential of Au-Ag alloys and explore glass transition and crystallization of $Ag_{50}Au_{50}$.

2 POTENTIAL OF ATOM

Within density function and quasi-atom concept[4], the dominant energy of the metal is viewed as the energy to embed an atom into the local electron density due to the remaining atoms of the system. The total energy of the system can be written as

$$E_{tot} = \sum_i E_i(\rho_{h,i}) + 1/2\sum_{i,j}\phi_{i,j}(R_{i,j}) \quad (1)$$

$$\rho_i = \sum_j f(r_{i,j}) \quad (2)$$

where ρ_i is total electron density at atom i due to the rest of the atoms in the system, and E_i is the embedding energy of placing an atom into that electron density. Finally, $\phi_{i,j}$ is short-range pair interaction representing the core-core repulsion, and $R_{i,j}$ is the

① [Foundation item] Project (50071028) supported by the National Natural Science Foundation of China
[Received date] 2001- 09- 07; [Accepted date] 2001- 12- 03

separation of the atom i and j.

In order to apply Eqn. 2, the electron density ρ_i, pair potential $\phi_{i,j}$ and embedding function E_i must be known. Knowledge related in detail can be found in Ref. [8]. It is necessary to make point that for AB alloy, the two-body potential of $\phi_{A-B}(R_{i,j})$ is obtained by

$$\phi_{A-B}(r)=\frac{1}{2}\left|\frac{f^A(r)}{f^B(r)}\phi^{A-A}(r)+\frac{f^B(r)}{f^A(r)}\phi^{B-B}(r)\right| \quad (3)$$

where $\phi^{A-A}(r)$ and $\phi^{B-B}(r)$ are the monatomic potentials. $f^A(r)$ and $f^B(r)$ are electronic density of A and B respectively.

3 PROCESS OF MOLECULAR DYNAMICS SIMULATION

Since the EAM energy implicitly includes many-body terms, the well developed theory of liquids interacting with pair potentials cannot be used. Thus molecular dynamics computer simulations have been performed to determine the predictions of the EAM for the liquid alloy structure and pressures. The MD simulations are performed in a cubic box subject to periodical boundary conditions for a system with 500 particles. It means that with repeating boundary conditions, one typically conducts a simulation with a box. Atoms that pass out one wall of the box pass back into the box through the opposite wall, thus at no time is an atom outside the box. This way there is no free surface, and the system simulates the bulk. The time step is 0.4 fs, the decline force method was used to decrease the temperature. We first run 2×10^4 time steps to keep the system in an balance state, then the liquid was cooled to 200 K at the rate of 4×10^{13} K/s and 4×10^{12} K/s respectively to examine the processing of amorphization and crystallization formation process. The configurations were recorded every 200 K. The atom volume and internal energy were reported every 10 K to explore the thermodynamics process during phase transition.

4 METHOD OF STRUCTURAL ANALYSES

4.1 Pair correlation function(PCF)

The pair correction function (PCF) $g(r)$ can be obtained by Fourier transformation of X-ray diffraction factor $S(Q)$. The $g(r)$ has been widely used to describe the structure characterization of liquid and amorphous states, it is defined as

$$g_{i,j}(r)=\frac{L^3}{N_iN_j}[(\sum_{\alpha=1}^{Ni}n_{\alpha j}(r))/4\pi r^2\Delta r] \quad (4)$$

where $g_{i,j}(r)$ is the probability of finding an atom in the range from r to $r+\mathrm{d}r$, L is the cell length of the box in the simulation, N_i and N_j are the number of atoms i and j respectively in the system, and $n_{\alpha j}$ is an averaged number of j-type atoms around I-type atoms in the sphere shell ranging from r to $r+\Delta r$, where Δr is the step of calculation.

As far as AB alloys, there would be three partial pair correction functions, namely $g_{A-A}(r)$, $g_{A-B}(r)$, $g_{B-B}(r)$, and one total PCF $g_{tot}(r)$.

4.2 Internal energy and atom volume

The internal energy of the system is the sum of potential and kinetic energy. The atom volume we refer to is the volume of the cubic box. In the constant-pressure simulations, the volume of the cubic box changes with temperature. The dependence of volume and the energy of the system on the temperature can reflect the phase transition.

4.3 Mean square displacement (MSD)

The mean square displacement of the particle in the MD can be described as

$$r^2(t)=\frac{1}{N}\sum_{i=1}^{N}|r_i(t)-r_i(0)|^2 \quad (5)$$

where t is the physical time in the MD simulation, N is the number of particle, $r_i(0)$ is the position vector of the ith particle for the system in its initial configuration, and $r_i(r)$ is the position vector of the ith particle at time t.

5 RESULTS AND DISCUSSION

5.1 Thermodynamics

Fig. 1(a) shows the internal energy versus the temperature. K_1 represents the cooling rate of 4×10^{13} K/s. The energy-temperature curve is nearly straight in the high and low temperature region. The change in energy is continuous. It is the typical feature of glass formation. The glass transition temperature T_g for a model system is defined by the temperature at the intersection of the extrapolations of the liquid and glassy plots. From Fig. 2, T_g is estimated to be 800 K or so. K_2 represents the cooling rate of 4×10^{12} K/s. From the curve, a sudden change in energy at the temperature about 800 K takes place. It shows that $Ag_{50}Au_{50}$ of super-liquid state becomes crystal when the cooling rate is K_2. We can conclude that the melting temperature is about 700 K that are well below the experimentally observed melting temperature. This would be attributed to the high cooling rate and to the finite size of our system. Obviously the lower the cooling rate is, the higher the melting temperature is during solidification.

5.2 Pair correlation function (PCF)

The structure of the system during rapid solidification is checked by examining physical parameter $g(r)$ of the atomic position. The partial PCF $g_{Au-Au}(r)$, $g_{Au-Ag}(r)$, $g_{Ag-Ag}(r)$ obtained at the rate of

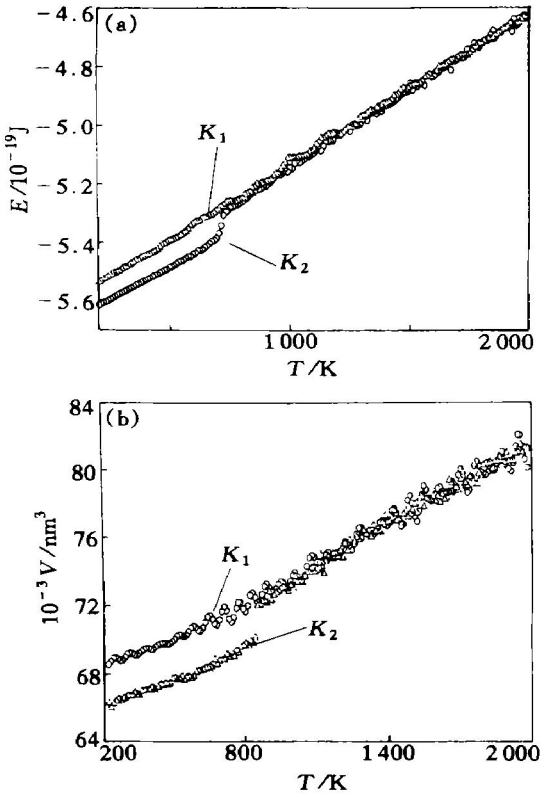

Fig. 1 Total energy (a) and volume (b) versus quenching temperature, K_1 and K_2 representing quenching processing at cooling rate of 4×10^{13} K/s, and 4×10^{12} K/s, respectively

4×10^{13} K/s are presented in Fig. 3. Obviously, $g_{Au-Ag}(r)$ has the maximum value among the three partial $g(r)$. This confirms that the heterogenic atom pairs have stronger interaction than those of the same atom pairs in Ag_{50}-Au_{50} liquid metals. Although the numbers of Ag particles is the same of Au particles in Ag_{50}-Au_{50} alloy, the $g_{Au-Au}(r)$, $g_{Ag-Ag}(r)$ are lower than those of $g_{Au-Ag}(r)$. This means that it is a possibility that Au atoms rather than Ag atoms occupy the near-neighbour coordination shell around the Ag atoms; and the Ag atoms occupy the near-neighbour coordination shell of Au atoms. The fact that the first peak becomes bigger and bigger with decreasing temperature indicates that during the cooling process, the ordering degree of liquid is strengthened. It is in accordance with the thermodynamic rule. As the temperature-quench becomes greater, the second peaks of the three kinds of PCF split into two subpeaks when the temperature is below 600 K, but they are not remarkable. The formation temperature of amorphous solid T_g is about 800 K. This means that the spliting temperature is lower than the glass transition temperature. From which we can conclude that the structure of disorder stack is not the only

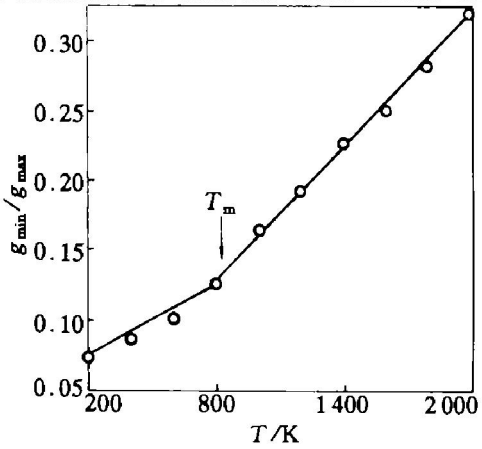

Fig. 2 Wendt-Abraham ratio g_{min}/g_{max} versus quenching temperature for $Ag_{50}Au_{50}$

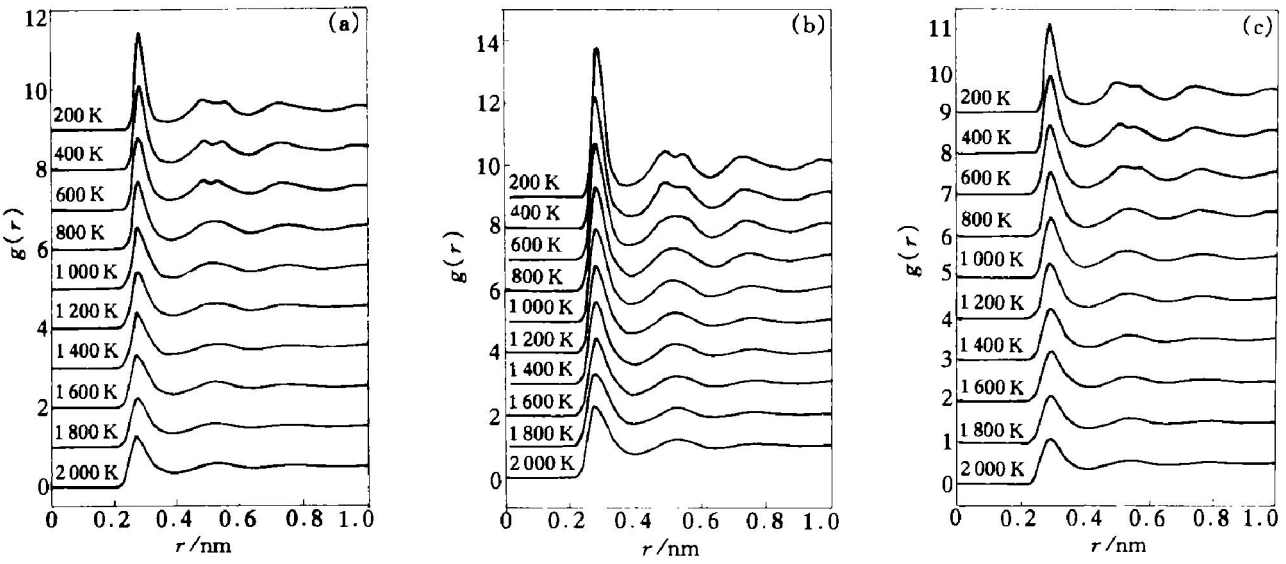

Fig. 3 Partial pair correlation function $g_{i,j}(r)$ versus r at different quenching temperatures during rapid solidification at cooling rate of 4×10^{13} K/s
(a) $-g_{Au-Au}(r)$; (b) $-g_{Au-Ag}(r)$; (c) $-g_{Ag-Ag}(r)$

configuration of amorphous solid. The partial PCF obtained at the cooling rate of 4×10^{12} K/s is shown in Fig. 4. The $g(r)$ values for liquid and supercooled liquid show similar behaviours as described above. However, solid states have different features. From Fig. 4, it can be seen that $g(r)$ shows peak structure characteristic of the crystal at low temperature. The $g(r)$ has a much higher peak than that in Fig. 3. It means that the chemical short-order is more strong. There appears a small peak between the first and second peak, and it becomes bigger and bigger with the decrease of temperature. This shows that the structure change happens, and a new structure forms in this temperature regions. From the three partial $g(r)$, we may say the liquid crystallize completely into FCC crystal. A little difference with the standard FCC crystal may be the reason why a small part of disorder structure exists in the crystal.

The total $g(r)$ of $Ag_{50}Au_{50}$ at the cooling rate of 4×10^{13} K/s and 4×10^{12} K/s are shown in Fig. 4. The remarkable difference of the two solidification production can be seen from Fig. 5 correctly. Fig. 5 (a) is the typical characteristics of glass state. The second peak splits at low temperature. The glass transition temperature can be determined using Wendt-Abraham parameter. The ratio of first minimum $g_{min}(r)$ and first maximum $g_{max}(r)$ of $g_{tot}(r)$ is shown in Fig. 2. The ratio is linear in both high and low temperature regions with respective slops. It is asserted the slop of the ratio as a function of temperature T changes at the glass transition. This is used to check the occurrence of the glass transition. In Fig. 2, the ratio obtained at cooling rate of 4×10^{13} K/s is given. Clearly, the ratio is linear with T at both high and low temperature. The line for high temperature intersects with that for low temperature at a temperature near 800 K. Fig. 5(b) shows the total $g(r)$ of $Ag_{50}Au_{50}$ at the cooling rate of 4×10^{12}K/s.

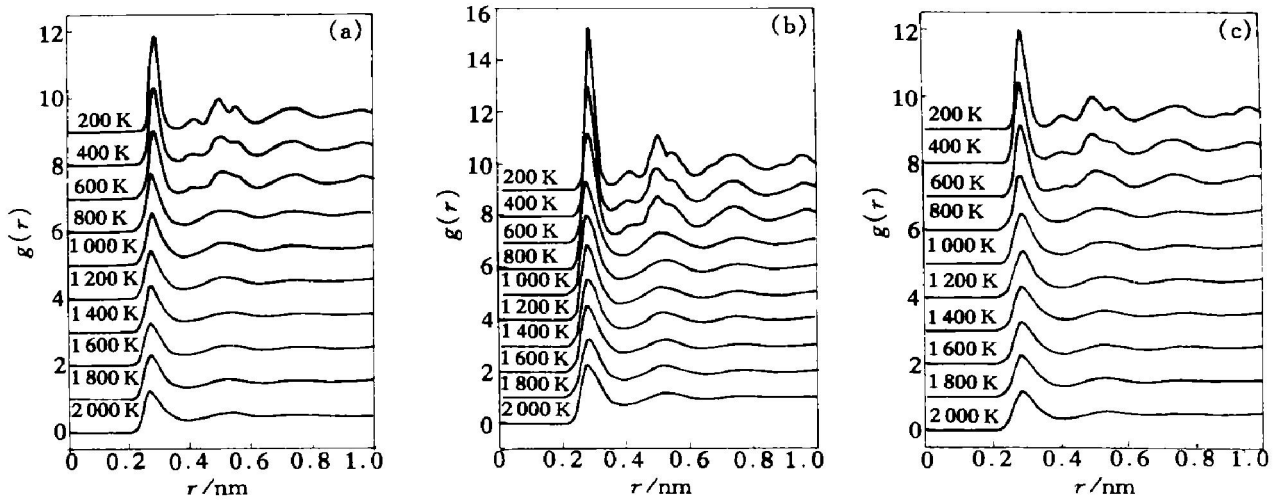

Fig. 4 Partial pair correlation function $g_{i,j}(r)$ versus r at different quenching temperatures during rapid solidification at cooling rate of 4×10^{12}K/s
(a) —$g_{Au-Au}(r)$; (b) —$g_{Au-Ag}(r)$; (c) —$g_{Ag-Ag}(r)$

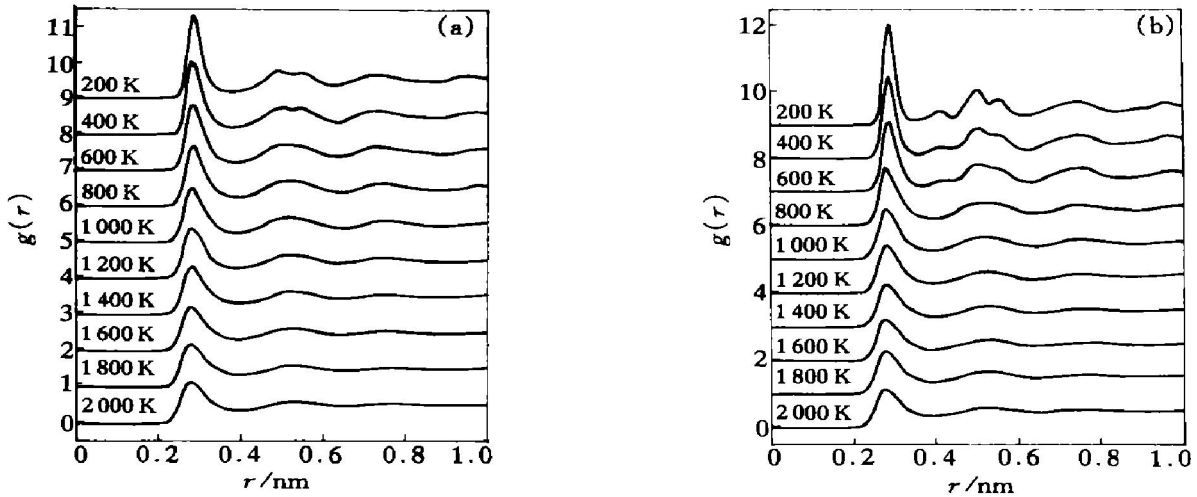

Fig. 5 Total pair correlation function $g(r)$ of $Ag_{50}Au_{50}$ versus r at different quenching temperatures during rapid solidification at different cooling rates
(a) —4×10^{13} K/s; (b) —4×10^{12} K/s

Accompanying with the decrease in temperature, various peaks become marked. It suggests that the system is in some kinds of regular structure. This demonstrates at this cooling rate, most atoms in the system crystallize into crystal. The $g(r)$ values for liquid and supercooled liquid show similar behaviours as described above.

5.3 Kinetics

The mean square displacements of $Ag_{50}Au_{50}$ were calculated from Eqn. 5 and displayed in Fig. 6 as a function of temperature. The rearrangement of atom positions is sensitive to the cooling rate during the solidification. The atom displacement increases largely in the liquid and superliquid at the relatively slow cooling rate. This means that the crystallization process is a diffusion process of atoms in a wide range and rearrangement process of atom positions. The change of MSD is very small during the formation of glass state. It suggests that atoms do not transfer in a wide range but move in a small range. The fact that liquid atoms gradually deviate from their original position until glass transition or crystallization tell us that quenched glass state are not merely frozen-fluid configurations, whereas the atoms are well localized as in the crystalline state.

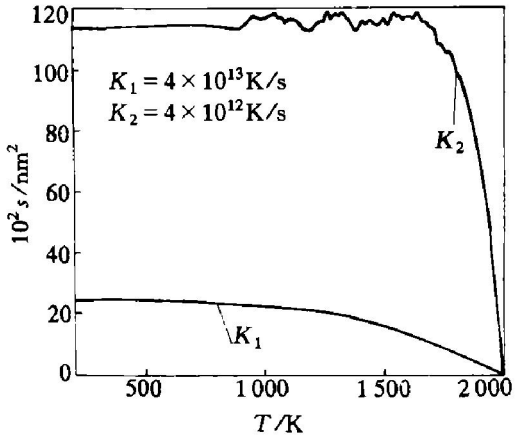

Fig. 6 Mean square displacement (s) of $Ag_{50}Au_{50}$ versus temperature during different rapid solidification processes

6 CONCLUSIONS

1) EAM function parameterized to bulk solid properties can correctly and efficiently predict the glass transition and crystallization of liquid metals during rapid solidification.

2) PCF show that the liquid $Ag_{50}Au_{50}$ crystallizes into a crystal at the cooling rate of 4×10^{12} K/s. Although the crystallization temperature simulated is lower than the experiment freezing point, it is reasonable EAM model describes the behavior of $Ag_{50}Au_{50}$ well.

3) Both the thermodynamic properties and the structure parameters predict the glass transition at the cooling rate of 4×10^{13} K/s, and the predicted glass transition temperature T_g is about 800 K.

4) MSD demonstrates that the glass state is not merely frozen liquid state but special structure; PCF manifests such features of liquid metal as short-range order and long-range disorder. The changes of PCF with the temperatures reflect the universal law of nature that liquid metal rises orderly and drops disorderly as the temperature lowers.

[REFERENCES]

[1] Massobric C, Pontikis V, Martin G. Molecular-dynamics study of amorphization by introduction of chemical disorder in crystalline $NiZr_2$[J]. Phys Rev, 1990, 41B(15): 10486.

[2] Walter K. Computer simulation of supercooled liquids and glasses[J]. J Phys Condens Matter, 1999, 11: R85-R115.

[3] Allen M P, Tildesley D J. Computer Simulation of Liquids [M]. New York: Oxford University Press, 1990.

[4] Daw M S, Baskes M I. Semiempirical, quantum mechanical calculation of hydrogen embrittlement in metals [J]. Phys Rev Lett, 1983, 50: 1285.

[5] Daw M S, Baskes M I. Embedded-atom method: derivation and application to impurities, surface, and other defects in metals [J]. Phys Rev, 1984, 29(12): 6443.

[6] Johnson R A. Analytic nearest-neighbor model for FCC metals [J]. Phys Rev, 1988, 37B: 3924.

[7] Johnson R A. Relationship between defect energies and embedded-atom-method parameters [J]. Phys Rev, 1988, 37B: 6121.

[8] Johnson R A. Alloy models with the embedded-atom method [J]. Phys Rev, 1989, 39B: 12554.

[9] Gomez M A, Chacon E. Structure and surface tension of the liquid-vapor interface of simple metals: a theoretical approach [J]. Phys Rev, 1992, 40B(2): 723.

[10] Holender J M. Molecular-dynamics studies of the thermal properties of the solid and liquid FCC metals Ag, Au, Cu and Ni using many-body interactions [J]. Phys Rev, 1990, 41B(12): 8054.

[11] Foiles S M, Baskes M I, Daw M S. Embedded-atom-method functions for the metals Cu, Ag, Au, Ni, Pd, Pt, and their alloys [J]. Phys Rev, 1986, 33B(12): 7983.

[12] Schonfeld B, Traube J, Kostorz G. Short-range order and pair potentials in Au-Ag [J]. Phys Rev, 1992, 45B(2): 613.

(Edited by HUANG Jin-song)